SynOpen R. Tiwari, M. Nath THIEME OPEN ACCESS Paper

A Divergent Approach to β-Pyrazine-Fused *meso*-Tetraphenyldiporphyrins

Raju Tiwari
Mahendra Nath*

Department of Chemistry, University of Delhi, Delhi-110007, India
mnath@chemistry.du.ac.in

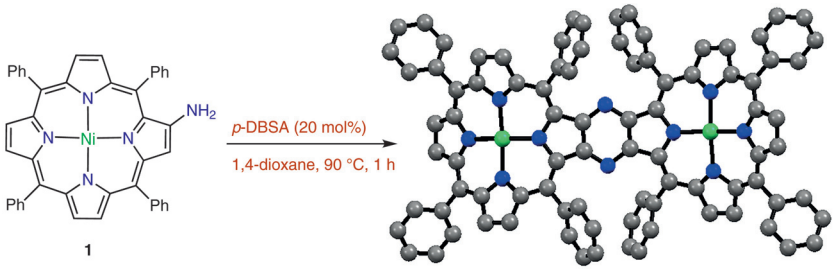

Received: 14.03.2018
Accepted after revision: 05.04.2018
Published online: 09.05.2018
DOI: 10.1055/s-0036-1591998; Art ID: so-2018-d0012-op

Abstract We describe an alternative methodology for the synthesis of β-pyrazine-fused diporphyrins in high yields from 2-amino-5,10,15,20-tetraphenylporphyrin nickel(II) derivatives by using *p*-dodecylbenzenesulfonic acid as an efficient Brønsted acid catalyst in 1,4-dioxane at 90 °C. The structural characterization, material morphology and electronic properties of the products are reported.

Key words Brønsted acid catalyst, *p*-DBSA, β-fused diporphyrins, electrochemistry, HOMO-LUMO energy gap, photophysical properties

β-Functionalized porphyrins with extended π-systems have received significant attention in recent decades due to their potential applications in optoelectronics, energy harvesting, electron-transfer processes and molecular devices.[1] Previously, a number of synthetic approaches including condensation of two chromophores,[2] stepwise fusion on the porphyrin periphery and a retro-Diels–Alder reaction[3] have been reported for the construction of diverse fused porphyrin analogues. Strategies such as oxidative annulation,[4] coupling[5] or metal-catalyzed reactions[6] are available to synthesize β-pyrazine fused diporphyrins, but some of these methodologies suffer from poor yields, tedious work-up procedures and the formation of unwanted side products. Therefore, a facile and efficient synthetic protocol for the synthesis of various π-extended pyrazine-fused diporphyrins from readily available starting materials is desirable so that the potential of these molecules can be exploited.

In the context of our efforts to develop new methodologies to construct β-functionalized porphyrins through peripheral functionalization of *meso*-tetraarylporphyrins,[7] we recently developed an efficient alternate method for the synthesis of β-pyrazine-fused *meso*-tetraphenyldiporphyrin nickel(II) derivatives through *p*-dodecylbenzenesulfonic acid (*p*-DBSA)-catalyzed dimerization of 2-amino-5,10,15,20-tetraphenylporphyrin nickel(II) (Scheme 1). The newly synthesized porphyrins showed excellent photophysical properties as their electronic absorption spectra were found to be redshifted with broadening or/and splitting in the Soret bands and revealed a reduction in the HOMO-LUMO energy gap.

Furthermore, a single-crystal analysis of β-pyrazine-fused *meso*-tetraphenyldiporphyrin nickel(II) (**3**) and electron microscopy showed a layered rectangular sheet (ca. 100 µm) type structure, which may be useful for various applications in material science. In this communication, we report the synthesis and characterization as well as photophysical and electrochemical studies of β-pyrazine-fused *meso*-tetraphenyldiporphyrin nickel(II) analogues.

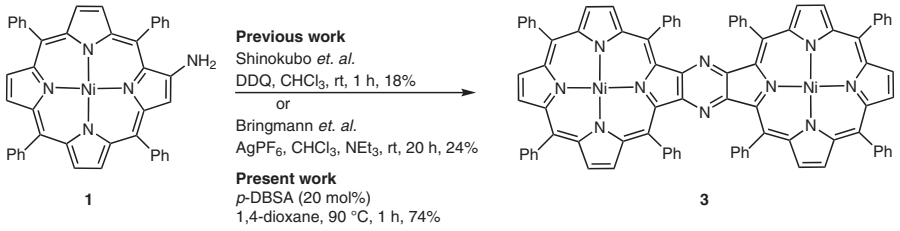

Scheme 1 Synthetic approaches to β-pyrazine-fused *meso*-tetraphenyldiporphyrin nickel(II) (**3**) from 2-amino-TPP (**1**)

Initially, the synthesis of β-pyrazine-fused *meso*-tetraphenyldiporphyrin nickel(II) (**3**) was attempted by heating 2-amino-5,10,15,20-tetraphenylporphyrin nickel(II) (**1**) in the presence of 5 mol% *p*-DBSA as Brønsted acid catalyst in 1,4-dioxane at 90 °C and the progress of reaction was monitored by TLC. After one hour, the formation of β-pyrazine-fused *meso*-tetraphenyldiporphyrin nickel(II) (**3**) was observed as a green spot on TLC along with starting material. Surprisingly, with time, no appreciable change was observed in the formation of the desired product. After the purification by column chromatography, the desired porphyrin product **3** was obtained in 7% yield (Table 1, entry 1). To improve the yield of **3**, attempts were made to optimize the reaction conditions by varying the catalyst load and reaction temperature (entries 2–9). The yield of the diporphyrin **3** increased on increasing the catalyst loading from 5 to 20 mol% (entries 1–4), but a further increase in catalyst loading resulted in a sharp decrease in the yield of diporphyrin **3** (entries 5–6) due to the conversion of starting material into an inseparable mixture of by-products. Similarly, the yield of diporphyrin **3** was decreased when the reactions were carried out at lower temperatures such as 25 and 60 °C (entries 7 and 8); while reaction at 100 °C provided the desired product in moderate yield (entry 9). Therefore, it was concluded that formation of diporphyrin **3** critically depends on the catalyst load and reaction temperature, with the optimum yield being obtained when the reaction was carried out with 20 mol% *p*-DBSA at 90 °C for one hour.

Under the optimized reaction conditions, β-pyrazine-fused *meso*-tetraphenyldiporphyrin nickel(II) analogues **3** and **4** were prepared[8] in 74% and 82% yields, respectively, by heating the corresponding precursors 2-amino-5,10,15,20-tetraphenylporphyrin nickel(II) (**1**) or 2-amino-12,13-dibromo-5,10,15,20-tetraphenylporphyrin nickel(II) (**2**) with 20 mol% *p*-DBSA in 1,4-dioxane at 90 °C for 1 hour (Scheme 2). Both the synthesized diporphyrins were characterized[9,10] spectroscopically. Interestingly, in the ^{1}H NMR spectra, twelve β-protons appeared as six doublets between 7.92 and 8.60 ppm with a coupling constant of 4.9 Hz and the *meso*-phenyl protons were observed between 7.12 and 8.08 ppm as multiplets. In the IR spectra (Figure ESI1), the disappearance of the NH_2 stretching band confirmed the conversion of the amino functionality into a pyrazine ring via the formation of a new C–N bond between the two porphyrin units. Finally, the structure of β-pyrazine-fused *meso*-tetraphenyldiporphyrin nickel(II) (**3**) was confirmed unambiguously by a single-crystal analysis.

Table 1 Optimization of Catalyst Load and Reaction Temperature for the Synthesis of Diporphyrin **3** from Nickel Complex of 2-Amino-TPP **1**[a]

Entry	*p*-DBSA (mol%)	Temp. (°C)	Yield (%)[b]
1	5	90	7
2	10	90	13
3	15	90	32
4	20	90	74
5	25	90	18
6	50	90	12
7	20	60	22
8	20	25	18
9	20	100	37

[a] All reactions were carried out in 1,4-dioxane for 1 hour.
[b] Isolated yields after column chromatography.

For single-crystal analysis, β-pyrazine-fused *meso*-tetraphenyldiporphyrin nickel(II) (**3**) was crystallized in chloroform by slow diffusion of MeOH at 298 K. The X-ray diffraction data were collected with an Oxford Diffraction Xcalibur CCD diffractometer with graphite-monochromated Mo-Kα radiation (λ = 0.71073 Å) at 298(2) K. The structure of β-pyrazine-fused *meso*-tetraphenyldiporphyrin nickel(II) (**3**) was solved by direct methods using SIR-92 and refined by full-matrix least-squares refinement techniques on F^2 using the SHELXL-97 program package in WinGX software. The non-hydrogen atoms such as carbon, nitrogen and chlorine were refined anisotopically and hydrogen atoms were placed into the calculated positions in the last cycle of the refinement. Thus, the structure of β-pyrazine-fused *meso*-tetraphenyldiporphyrin nickel(II) **3** was established as presented in Figure 1.[11] Interestingly, β-pyrazine-fused *meso*-tetraphenyldiporphyrin nickel(II) (**3**) exhibits a nonplanar (Saddle-shaped) conformation in which the pyrrole rings are alternately displaced above and below the mean plane of the 24-atom core and the central nickel atom adopts a slightly distorted square-planar geometry after the formation of β,β′-pyrazine-fused ring.

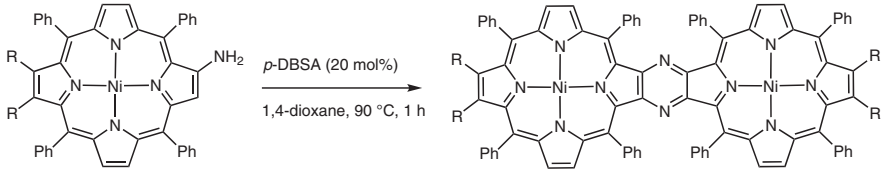

1: R = H
2: R = Br

3: R = H, 74%
4: R = Br, 82%

Scheme 2 Synthesis of β-pyrazine-fused *meso*-tetraphenyldiporphyrins **3** and **4**

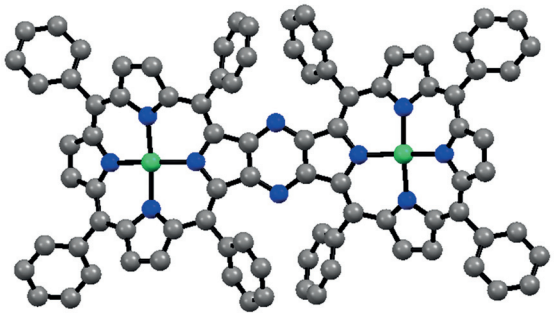

Figure 1 Single-crystal structure of β-pyrazine-fused *meso*-tetraphenyldiporphyrin nickel(II) (**3**). Hydrogen atoms and solvent molecules are omitted for clarity.

The single-crystal parameters and refinement data of β-pyrazine-fused *meso*-tetraphenyldiporphyrin nickel(II) (**3**) are listed in Table ESI1. In particular, the triclinic crystal system with cell parameters: a = 11.0254(16), b = 14.193(2), c = 14.762(2) Å, α = 62.215(17)°, β = 89.607(13)° and γ = 84.568(13)° in space group P-1 was found for β-pyrazine-fused *meso*-tetraphenyldiporphyrin nickel(II) (**3**). Furthermore, **3** has an inversion center in the middle of the pyrazine ring and the central nickel atom is slightly displaced towards the N3 from the central position.[4,5]

The wire-frame and space-filling packing diagrams of the crystal structure of β-pyrazine-fused *meso*-tetraphenyldiporphyrin nickel(II) (**3**), as viewed along the b-axis are presented in Figure ESI3. The two half-molecules of diporphyrin **3** are found within the unit cell and therefore the total contribution to one unit cell is 1, thus justifying Z = 1 (Table ESI1). In addition, the space-filling model clearly demonstrates the presence of voids within the unit cell. Calculations were performed using Olex2 crystallographic software package and various visualizing models such as 2D view, surface view and point view (Figure ESI4) were developed that clearly show the presence of voids in the crystal lattice of **3**. Among these voids, the largest spherical void present in the crystal lattice occupies a volume of 23.4 Å^3. However, the volumes occupied by **3** and solvent molecules (chloroform) were found to be 931.5 Å^3 and 895.5 Å^3, respectively.

The short-range interactions between different atoms present in the crystal lattice of **3** are shown with different colors in Figure ESI5. In particular, three types of interactions have been shown; π-π stacking and dipole-dipole interactions as expected due to the presence of two (18+4) π-electron porphyrin systems and the chloroform (solvent) molecules in the crystal lattice. In Figure ESI5, the red color represents the interactions between *meso*-phenyl H (H29) and β-carbon (C6), the blue color represents the interactions between β-carbons (C12-C12) and the green color represents the interactions among the chloroform H (H108) and pyrrole ring atoms (N2, C6, and C9). Among these, the interactions between β-carbons (C12-C12; blue color) are purely π-π stacking as the distance between interacting centers (C12-C12) is 3.39 Å. The remaining interactions (shown by red and green colors) are dipole-dipole interactions as the distance between interacting centers is found to be in the range 2.43–2.89 Å.

Interestingly, when a 2D network model of **3** was developed using Mercury software based on short-range interactions, it was observed that **3** interacts with four other molecules of diporphyrin **3** along with two chloroform molecules as shown in Figure 2.

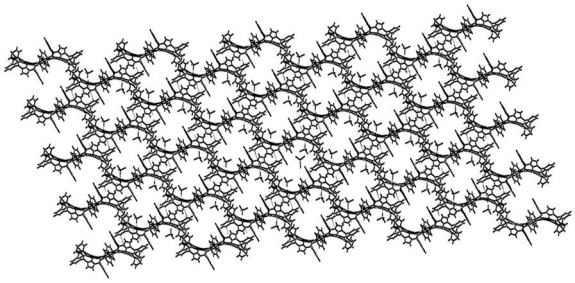

Figure 2 2D network of β-pyrazine-fused *meso*-tetraphenyldiporphyrin nickel(II) **3** based on short-range interactions

The morphology of **3** was also analyzed by scanning electron microscopy, which revealed layered rectangular sheet like structures with dimensions of 150×80×20 μm. Additionally, these rectangular sheets exhibit a rough surface area and cracks with dimensions of 80×0.2 μm (Figure 3).

The UV/Vis spectra of β-pyrazine-fused *meso*-tetraphenyldiporphyrins **3** and **4** were recorded in dichloromethane at 25 °C (Figure 4). Interestingly, the electronic absorption spectrum of **3** displayed split and redshifted Soret bands between 420–490 nm in addition to two redshifted Q bands at 577 and 610 nm in comparison to NiTPP (Soret 417 nm, Figure 5). However, β-pyrazine-fused 12,13,12′,13′-tetrabromo-5,10,15,20-tetraphenyldiporphyrin nickel(II) **4** showed two well-separated Soret bands at 432 and 490 nm and two redshifted Q bands at 581 and 629 nm in comparison to both NiTPP and diporphyrin **3**. The appearance of a diffuse shoulder with the Soret band in the spectrum of **3** clearly indicates the presence of some perturbation in the ground state. The redshifted Soret and Q bands of β-pyrazine-fused *meso*-tetraphenyldiporphyrin nickel(II) analogues **3** and **4** in comparison to nickel(II) 5,10,15,20-tetraphenylporphyrin may be accounted for by extended π-conjugation and decrease in HOMO-LUMO energy gap.[4–6,12]

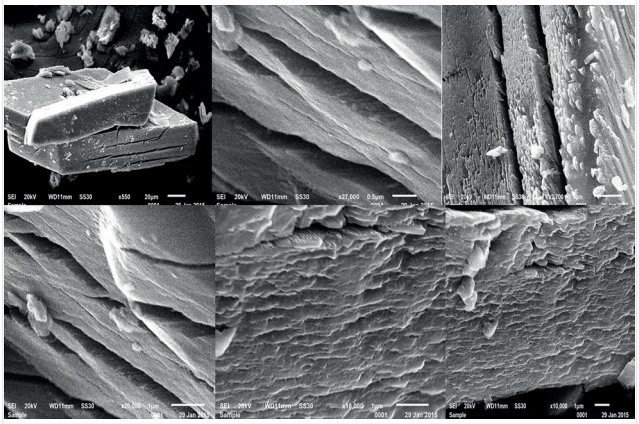

Figure 3 SEM images of β-pyrazine-fused *meso*-tetraphenyldiporphyrin nickel(II) **3**

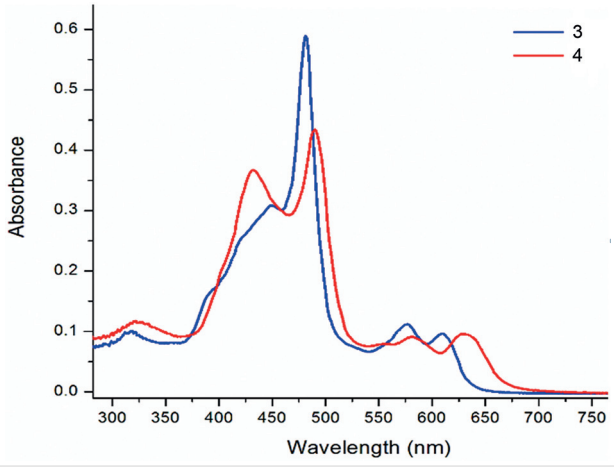

Figure 4 UV/Vis spectra of β-pyrazine-fused *meso*-tetraphenyldiporphyrins **3** and **4** in CH_2Cl_2 (1×10^{-6} mol L^{-1}) at 25 °C

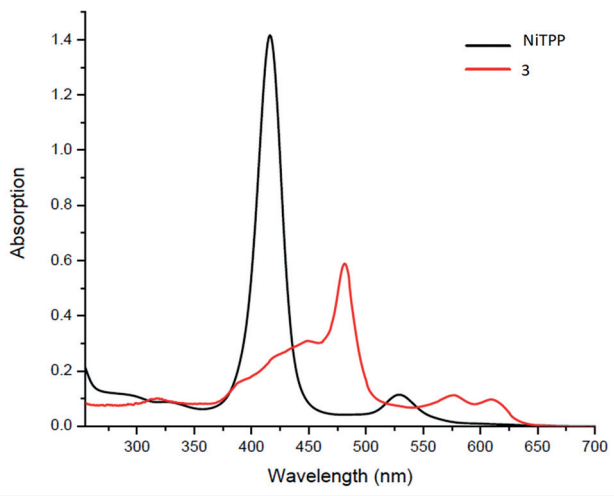

Figure 5 UV/Vis spectra of NiTPP and β-pyrazine-fused *meso*-tetraphenyldiporphyrin **3** in CH_2Cl_2 (1×10^{-6} mol L^{-1}) at 25 °C

The oxidation and reduction behavior of porphyrins **3** and **4** were studied using three electrodes (glassy carbon, platinum wire and Ag/AgCl as working, counter and reference electrode, respectively) by cyclic voltammetry in dichloromethane solution containing *tetra-n*-butylammoniumhexafluorophosphate (TBAH) as supporting electrolyte at 25 °C; the data are presented in Table 2.[13] Porphyrins **3** and **4** showed four oxidation peaks between 0.80 and 1.51 V and two reduction peaks between –1.22 and –1.72 V (Table 2). The appearance of four oxidation peaks showed that the two porphyrin units behave as two equivalent units and interacting redox centers.[5] Notably, the separation between the last two $E_{1/2,\,ox}$ [$E_{1/2,\,ox4} - E_{1/2,\,ox3}$ = 260 mV and 370 mV for **3** and **4**, respectively] is greater than first two $E_{1/2,\,ox}$ [$E_{1/2,\,ox2} - E_{1/2,\,ox1}$ = 230 mV and 140 mV for **3** and **4**, respectively]; following similar trends to those observed for a zinc derivative.[5] Interestingly, the formation of a fused pyrazine ring and extension of π-conjugation has affected the HOMO orbitals as the first oxidation potentials decreased by 240 mV in comparison to NiTPP (1.07 V).[14] Therefore, it may be concluded that the energy of the HOMO orbitals increases after the formation of β-pyrazine-fused *meso*-tetraphenyldiporphyrin nickel(II) analogues **3** and **4**. As a result, a reduction in the HOMO-LUMO energy gap and bathochromic shifts in the UV/Vis spectra are observed in the case of these diporphyrins. Furthermore, the optical energy gap (Q_x) and electrochemical energy gap (HOMO-LUMO gaps) were calculated, which also support the decrease in the HOMO-LUMO energy gap (Table 2).

Table 2 Cyclic Voltammetry Data of Diporphyrins **3** and **4** in CH_2Cl_2[a]

Porphyrins	Oxidation ($E_{1/2}$, V)	Reduction ($E_{1/2}$, V)	HOMO-LUMO gap (V)[b]	Q_x (0,0) (eV)[c]
3	1.49, 1.23, 1.06, 0.83	–1.22, –1.68	2.05	2.03
4	1.51, 1.14, 0.94, 0.80	–1.22, –1.72	2.02	2.00

[a] Half-wave potentials ($E_{1/2}$) in volt vs Ag/AgCl at scan rate of 50 mV/s containing *tetra-n*-butylammoniumhexafluorophosphate as supporting electrolyte (0.1 M) at 25 °C
[b] Calculated as the difference between the first oxidation and reduction potentials.
[c] Calculated as $1241/\lambda_{max}$ nm.

In conclusion, an alternative methodology has been developed for the synthesis of β-pyrazine-fused *meso*-tetraphenyldiporphyrin nickel(II) derivatives from readily available 2-amino-5,10,15,20-tetraphenylporphyrins. On photophysical and electrochemical investigations, these porphyrins showed extension of π-conjugation, bathochromic shifts and decreased oxidation potentials compared to their precursors. These results may be useful in designing π-extended porphyrin architectures for electronic and material applications.

Funding Information

R.T. is grateful to CSIR, New Delhi, India, for an SRF-NET Fellowship. Moreover, we gratefully acknowledge the award of a R&D grant from University of Delhi, Delhi, India.

Acknowledgment

The authors are grateful to CIF, University of Delhi, India, for providing ^{1}H NMR, SEM and single crystal X-ray data. We are also thankful to Prof. R. Nagarajan for extending support to use the cyclic voltammetry instrument funded by the DU-DST PURSE grant. R.T. is grateful to CSIR, New Delhi, India, for an SRF-NET Fellowship.

Supporting Information

Supporting information for this article is available online at https://doi.org/10.1055/s-0036-1591998.

References

(1) (a) Vicente, M. G. H.; Jaquinod, L.; Smith, K. M. *Chem. Commun.* **1999**, 1771. (b) Anderson, H. L. *Chem. Commun.* **1999**, 2323. (c) Arnold, D. P. *Synlett* **2000**, 296. (d) Burrell, A. K.; Officer, D. L. *Synlett* **1998**, 1297. (e) Holten, D.; Bocian, D. F.; Lindsay, J. S. *Acc. Chem. Res.* **2002**, *35*, 57. (f) Kim, D.; Osuka, A. *Acc. Chem. Res.* **2004**, *37*, 735. (g) Hwang, I. W.; Aratani, N.; Osuka, A.; Kim, D. *Bull. Korean Chem. Soc.* **2005**, *26*, 19. (h) Kim, D.; Osuka, A. *J. Phys. Chem. A* **2003**, *107*, 8791. (i) Tanaka, T.; Osuka, A. *Chem. Soc. Rev.* **2015**, *44*, 943. (j) Sharma, R.; Gautam, P.; Shaikh, M. M.; Mishra, R. *Dalton Trans.* **2013**, *42*, 5539. (k) Sharma, R.; Gautam, P.; Mishra, R.; Shukla, S. K. *RSC Adv.* **2015**, *5*, 27069.

(2) (a) Crossley, M. J.; King, L. G. *J. Chem. Soc., Chem. Commun.* **1984**, 352. (b) Crossley, M. J.; Burn, P. L. *J. Chem. Soc., Chem. Commun.* **1987**, 39. (c) Crossley, M. J.; Burn, P. L. *J. Chem. Soc., Chem. Commun.* **1991**, 1569. (d) Crossley, M. J.; Govenlock, J. L.; Prashar, J. K. *J. Chem. Soc., Chem. Commun.* **1995**, 2379. (e) Crossley, M. J.; Johnston, L. A. *Chem. Commun.* **2002**, 1122. (f) Khoury, T.; Crossley, M. J. *Chem. Commun.* **2007**, 4851.

(3) (a) Uno, H.; Hahimoto, M.; Fujimoto, A. *Heterocycles* **2009**, *77*, 887. (b) Uno, H.; Nakamoto, K.; Kuroki, K.; Fujimoto, A.; Ono, N. *Chem. Eur. J.* **2007**, *13*, 5773. (c) Ito, S.; Nakamoto, K.; Uno, H.; Murashima, T.; Ono, N. *Chem. Commun.* **2001**, 2696.

(4) Akita, M.; Hiroto, S.; Shinokubo, H. *Angew. Chem. Int. Ed.* **2012**, *51*, 2894.

(5) Mandoj, F.; Nardis, S.; Pudi, R.; Lvova, L.; Fronczek, F. R.; Smith, K. M.; Prodi, L.; Genovese, D.; Paolesse, R. *Dyes Pigm.* **2013**, *99*, 136.

(6) Bruhn, T.; Witterauf, F.; Gotz, D. C. G.; Grimmer, C. T.; Wurtemberger, M.; Radius, U.; Bringmann, G. *Chem. Eur. J.* **2014**, *20*, 3998.

(7) (a) Nath, M.; Huffman, J. C.; Zaleski, J. M. *J. Am. Chem. Soc.* **2003**, *125*, 11484. (b) Nath, M.; Huffman, J. C.; Zaleski, J. M. *Chem. Commun.* **2003**, 858. (c) Nath, M.; Pink, M.; Zaleski, J. M. *J. Am. Chem. Soc.* **2005**, *127*, 478. (d) Boerner, L. J. K.; Nath, M.; Pink, M.; Zaleski, J. M. *Chem. Eur. J.* **2011**, *17*, 9311. (e) Nath, M.; Pink, M.; Zaleski, J. M. *J. Organomet. Chem.* **2011**, *696*, 4152. (f) Sharma, S.; Nath, M. *New J. Chem.* **2011**, *35*, 1630. (g) Sharma, S.; Nath, M. *J. Heterocycl. Chem.* **2012**, *49*, 88. (h) Sharma, S.; Nath, M. *Dyes Pigm.* **2012**, *92*, 1241. (i) Bhatt, R. K.; Sharma, S.; Nath, M. *Monatsh. Chem.* **2012**, *143*, 309. (j) Sharma, S.; Nath, M. *Beilstein J. Org. Chem.* **2013**, *9*, 496. (k) Singh, D. K.; Nath, M. *Org. Biomol. Chem.* **2015**, *13*, 1836. (l) Tiwari, R.; Nath, M. *New J. Chem.* **2015**, *39*, 5500. (m) Tiwari, R.; Nath, M. *Dyes Pigm.* **2018**, *152*, 161.

(8) **Synthesis of β-pyrazine-fused *meso*-tetraphenyldiporphyrin nickel(II) analogues 3 and 4**
To a solution of 2-amino-5,10,15,20-tetraphenylporphyrin nickel(II) (**1**; 68.5 mg, 0.1 mmol) or 2-amino-12,13-dibromo-5,10,15,20-tetraphenylporphyrin nickel(II) (**2**; 84.4 mg, 0.1 mmol) in 1,4-dioxane (10 mL), *p*-dodecylbenzenesulfonic acid (6.52 mg, 0.02 mmol) was added. The reaction mixture was stirred at 90 °C for one hour and the progress of reaction was monitored by TLC. After completion of the reaction, the mixture was diluted with ethyl acetate (40 mL) and washed with water (2 × 40 mL). The organic layer was collected and dried over anhydrous sodium sulfate. After filtration, the solvent was evaporated and the crude product was purified by silica gel column chromatography, eluting with 25% chloroform in hexane. The purified product was recrystallized from chloroform/methanol (1:1) solution.

(9) **Analytical data for β-pyrazine-fused *meso*-tetraphenyldiporphyrin nickel(II) (3):** Green solid; yield: 50.5 mg (74%); IR (KBr): 2919, 2850, 1596, 1460, 1442, 1352, 1286, 1178, 1139, 1075, 1008, 909, 831, 797, 750, 717, 699 cm^{-1}; ^{1}H NMR (400 MHz, $CDCl_3$): δ = 8.60 (d, *J* = 4.9 Hz, 2 H, β-pyrrolic H), 8.59 (d, *J* = 4.9 Hz, 2 H, β-pyrrolic H), 8.52 (d, *J* = 4.9 Hz, 2 H, β-pyrrolic H), 8.49 (d, *J* = 4.9 Hz, 2 H, β-pyrrolic H), 8.02 (d, *J* = 4.9 Hz, 2 H, β-pyrrolic H), 7.92 (d, *J* = 4.9 Hz, 2 H, β-pyrrolic H), 8.08–7.91 (m, 10 H, *meso*-phenyl H), 7.66–7.58 (m, 18 H, *meso*-phenyl H), 7.41–7.22 (m, 4 H, *meso*-phenyl H), 7.32–7.30 (m, 4 H, *meso*-phenyl H), 7.22–7.12 (m, 4 H, *meso*-phenyl H); UV/Vis (CH_2Cl_2): λ_{max} (ε × 10^{-3}) = 422 (186.6), 449 (225.9), 481 (429.3), 577 (80.0), 610 (69.6) nm; MALDI-TOF MS: *m*/*z* [M$^+$] calcd for $C_{88}H_{52}N_{10}Ni_2$: 1364.30; found: 1364.30.

(10) **Analytical data for β-pyrazine-fused 12,13,12′,13′-tetrabromo-5,10,15,20-tetraphenyldiporphyrin nickel(II) (4).** Grey-green solid; yield: 68.7 mg (82%); IR (KBr): 2924, 1588, 1347, 1055, 1015, 791, 749, 697 cm^{-1}; ^{1}H NMR (400 MHz, $CDCl_3$): δ = 8.59–8.26 (m, 8 H, β -pyrrolic H), 8.08–7.87 (m, 6 H, *meso*-phenyl H), 7.84–7.79 (m, 4 H, *meso*-phenyl H), 7.66–7.62 (m, 18 H, *meso*-phenyl H), 7.47–7.46 (m, 4 H, *meso*-phenyl H), 7.31–7.29 (m, 4 H, *meso*-phenyl H), 7.18–7.17 (m, 4 H, *meso*-phenyl H); UV/Vis (CH_2Cl_2): λ_{max} (ε × 10^{-3}) = 432 (366.8), 490 (433.7), 581 (91.5), 629 (96.1) nm; MALDI-TOF MS: *m*/*z* [M$^+$] calcd for $C_{88}H_{48}N_{10}Ni_2Br_4$: 1675.95; found: 1675.95.

(11) Crystallographic data for β-pyrazine-fused *meso*-tetraphenyldiporphyrin nickel(II) (**3**) have been deposited with the Cambridge Crystallographic Data Centre as supplementary publication data CCDC-1043957

(12) (a) Ventura, B.; Flamigni, L.; Marconi, G.; Lodato, F.; Officer, D. L. *New J. Chem.* **2008**, *32*, 166. (b) Gouterman, M. *J. Mol. Spectrosc.* **1961**, *6*, 138. (c) Spellane, P. J.; Gouterman, M.; Antipas, A.; Kim, S.; Liu, Y. C. *Inorg. Chem.* **1980**, *19*, 386.

(13) The electrochemical data were obtained by using a three-electrode CHI 600 D electrochemical analyser, USA. Glassy carbon, platinum wire and Ag/AgCl electrode were used as working, counter and reference electrodes, respectively

(14) (a) Dolphin, D.; Niem, T.; Felton, R. H.; Fujita, I. *J. Am. Chem. Soc.* **1975**, *97*, 5288. (b) Johnson, E. C.; Niem, T.; Dolphin, D. *Can. J. Chem.* **1978**, *56*, 1381.